Fate of phosphorus and potassium in single-pellet thermal conversion of forest residues with a focus on the char composition

Ali Hedayati [a],[*], Torbjörn A. Lestander [b], Magnus Rudolfsson [b], Mikael Thyrel [b], Marcus Öhman [a]

[a] Luleå University of Technology, Energy Engineering, Division of Energy Science, SE-971 87, Luleå, Sweden
[b] Swedish University of Agricultural Sciences, Department of Forest Biomaterials and Technology, SE-901 83, Umeå, Sweden

ABSTRACT

The phosphorus and potassium contents of the char obtained from thermal conversion of forest residues can limit its utilization as an alternative fuel and reducing agent to substitute coal/coke in the steelmaking industry. In this study, ash transformation and release of K and P during single-pellet thermal conversion of different types of forest residues (i.e., bark, twigs, and bark+twigs) were investigated with the aid of a vertical tube furnace (Macro-TGA) at different temperatures (i.e., 600, 800, and 950 °C) and within and after different fuel conversion stages, i.e., devolatilization and char gasification. The residual char before and after full devolatilization, and ash after char gasification were characterized by SEM-EDS, XRD, and ICP-OES with the support of thermochemical equilibrium calculations. The concentrations of K (7970–19500 mg/kg) and P (1440–4925 mg/kg) in the char produced after devolatilization were more than four times higher than in coke and pulverized coal frequently used in metallurgical processes. A low amount of P and K ($\leq$15%) were released from all fuels. K and P were evenly distributed within the char residues, and no crystalline compounds containing K and P were found. In ash residues of bark, K was found in $K_2Ca_2(CO_3)_3$, and $K_2Ca(CO_3)_2$. K in ash residues from twigs and bark+twigs was mainly found in the amorphous part of ash, most likely in the form of K-Ca rich silicates. Apatite was found as the main P crystalline compound in all ashes at all temperatures. Estimations show that a release of more than 80% is needed for the studied forest residual assortments to reach K and P concentrations typical of blast furnace coals and cokes.

1. Introduction

Shifting from fossil fuels to alternative fuels is considered a promising strategy to mitigate global warming caused by emissions of greenhouse gases, among them carbon dioxide (CO_2). The use of coal and coke in the steel industry is one of the major industrial contributors to CO_2 emissions and accounts for approximately 4–7% of worldwide emissions [1]. Although biomass from plants is being considered as a viable alternative to replace reducing agents such as coal and coke in steelmaking, utilization of untreated biomass has several limitations such as high volatile and moisture content, low heating value and energy density, and high concentrations of undesired inorganic elements (e.g., potassium (K) and phosphorus (P)). Therefore, thermal pre-treatment of biomass in order to obtain an upgraded fuel (herein called char) is crucial and inevitable [1]. Previous studies [1,2] showed that among all possible thermal treatments of biomass, pyrolysis/gasification of biomass at temperatures above 500 °C to obtain a reasonable yield of

char (15–30%), is a promising method to produce an upgraded fuel that potentially can be used as a metallurgical reducing agent.

Pyrolysis has traditionally been carried out in batch operation facilities with energy efficiencies as low as 10% [3]. More modern facilities operate a continuous process operation utilizing screw reactors, rotary kilns, and fixed bed reactors [4,5]. Although pyrolysis of biomass improves some of the char properties, such as reducing moisture content, bulk volume and increasing heating value and energy density, it may also increase K and P concentrations when the original mass decreases due to the mass loses of char. This may limit the utilization of the biobased char as an alternative fuel and reducing agent in the iron and steel making industry. K, which is abundant in most biomasses from plants, can reduce the strength of iron ore pellets in blast furnaces, impede the gas flow, negatively impact refractory materials, promote the formation of scaffolds, and give rise to increased consumption of the reducing agent in a blast furnace [1,6,7]. There are also expenses associated with downstream refining processes to remove P, as it impairs

the mechanical properties of steel. Hence, the fuels and reducing agents to be used in steel making should preferably have low P content [1,8,9].

Forest-based biomass from boreal forests consisting mostly of conifers is a potentially promising alternative feedstock to utilize in the iron and steel industry because its content of non-desirable elements is usually lower than in other types of biomass, such as agricultural residues [1,10–12]. Among all forest-based biomasses, stem wood is probably the most suitable, since its ash content and its amount of harmful elements is lower than in the coal and coke used in metallurgical processes today [1]. There is, however, growing competition for stem wood-based fuel feedstocks as the use of bio-based transportation fuels and materials also increases [3]. Therefore, forest residues should be studied for use in char production due to high availability and relatively low costs [13,14]. As these forest residues have a higher concentration of K and P compared to coal and coke [10], the char produced from these feedstocks may contain excessively high concentrations of these elements.

Forest residues usually consist of different parts of the tree such as bark, branches, and foliage. Tree species, tree parts, tree age, and the harvesting season may all have a significant effect on the content of the ash-forming elements, as well as their distributions and associations with the organic matrix [15]. For example, twigs of spruce consist mainly of needles, but also small parts of bark, and wood, each of which have different distributions of critical ash-forming elements and different associations with the organic part. Needles are rich in Ca, Si, and K and have relatively high P content, bark is rich in Ca, and K and have moderate P content, while stem wood has a low content of Ca and K, and a very low P content. Werkelin et al. [15,16] showed that the contents of K and P were strongly correlated with each other in forest residues. In general, the K and P contents are high in branches; however, the P content is lower than the K content. In this kind of biomass, the majority of P ($\sim$75%) is found in the form of organically-bound phosphates that are mainly water-soluble, while the rest is covalently bonded to the organic matrix, which is acid-soluble [16]. The majority of K ($\sim$75%) is present as free ions, which can be extracted by water and the rest is ionically bonded to the organic matrix [16].

Previous studies [17–20] on the thermal conversion of forest-based biomass have shown that only small fractions of K are released at low temperatures (<700 °C). Depending on the process temperature and char conversion time, the main fraction of K can be found in different chemical forms in the char, such as organically-associated K, K-Ca carbonates, K sulfates, and K silicates [17]. Detailed studies of ash transformation and release of P in thermal conversion of forest-based biomass are rarely found in the literature. Previous work has suggested, though, that the majority of P is expected to form hydroxyapatite ($Ca_5(PO_4)_3OH$) or Ca-whitlockite (β-$Ca_3(PO_4)_2$) during thermal conversion of forest-based biomass [21]. Most studies on the release and ash transformation of critical elements in biomass during thermochemical conversion limited their focus to the fate of Si, K, Ca, S, and Cl under combustion conditions [22–26]. Considerably fewer studies [27–29] were conducted under pyrolysis and gasification conditions, and these studies are mainly limited to a specific type of agricultural biomass such as straw from wheat, rice, and corn. It is important to address the limited knowledge of ash transformation reactions and release of P and K in thermal processing of forest residues, in order to assess the suitability of the char for utilization in steelmaking processes.

Therefore, the main objective of this study was to determine the ash transformation and release of critical ash-forming elements, specifically P and K, during single-pellet thermal conversion of forest residues. Special focus was set on the P and K concentration and speciation in the produced char residues. Residual char and ash were characterized within and after different fuel conversion stages, i.e., devolatilization and char gasification, and the results were interpreted with the support of thermochemical equilibrium calculations (TECs). Fuels representing a wide range of ash compositions in forest residue assortments were used, i.e., bark (rich in Ca and K with lower P content), twigs (mainly needles

but also some bark and wood from fine terminal branches) (rich in Si, Ca, K with higher P content) from typical softwood species, and a mixture of bark and twigs (rich in Si, Ca, K rich with moderate P content).

2. Materials and methods

2.1. Fuels

Twigs and bark from Norway spruce (*Picea abies* Karst. (L.)) trees were collected in Umeå, Sweden (63°48′43.3″N 20°14′07.9″E) and dried at 60 °C before milling in a hammer mill (Kamas Industri AB, Malmö, Sweden) over a 5 mm sieve. Twigs, bark and a mix of equal parts (dry matter) twigs and bark were thereafter pelletized at a moisture content of 10% in a Mini Pellet Mill (Farm Feed Systems LTD, Cinderford, UK) with a rotating die and a compression ratio of 20:6. The fuels produced for the experiments were cylindrical pellets 6 mm in diameter with a weight of 700 ± 10 mg after adjusting the length. Table 1 shows the fuel composition with respect to proximate and ultimate analysis, and the concentration of main ash-forming elements. The elemental analysis of the fuel was performed on three different samples (10–15 g) taken from different parts of the 3–5 kg fuel batches, in order to obtain representative samples. The used fuels represent a wide range of ash composition within forest residues from a typical species representing boreal forests in one of the largest terrestrial biomes. The bark contained a high amount of cations (K+Ca+Mg) and a low amount of anions (Si+P), while twigs contain a high amount of both cations and anions (K+Ca+Mg vs. Si+P). Comparing elemental compositions of bark and twigs, concentrations of K, Si, and P in twigs are higher than in bark while the concentration of Ca in the bark is higher than in twigs.

2.2. Experimental procedure

Fig. 1 shows a schematic sketch of the single-pellet reactor (Macro-

Table 1
Fuel characteristics (average of three samples $\pm$ standard deviation).

	Analytical standard	Bark	Bark+Twigs (50:50)	Twigs
Proximate Analysis				
Moisture content (wt% w.b.[a])	ISO 18134	5	3.4	4.8
Volatile matter (wt% d.b.[b])	ISO 18123	74.8	75.1	75.4
Ash content at 550 °C (wt% d. b.[b])	ISO 18122	3.3	3.6	4.1
Ultimate Analysis (wt% d.b.)				
C	ISO 16948	51.8	51.7	51.6
H	ISO 16948	6.1	6.2	6.4
N	ISO 16948	0.3	0.7	1
O	Calculated	38.5	37.7	36.8
Cl	ISO 16994	0.0131 ± 0.0002	0.0245 ± 0.0011	0.0307 ± 0.0004
S	ISO 16967	0.0315 ± 0.0009	0.0542 ± 0.0019	0.0644 ± 0.0005
Elemental Analysis Major Ash Forming Elements (mg/kg d.b.)				
Al	ISO 16967	235 ± 4	289 ± 7	373 ± 4
Ca	ISO 16967	9307 ± 208	7423 ± 65	6206 ± 33
Fe	ISO 16967	118 ± 1	158 ± 5	226 ± 2
K	ISO 16967	2463 ± 26	3327 ± 64	4333 ± 29
Mg	ISO 16967	863 ± 12	965 ± 8	771 ± 5
Mn	ISO 16967	302 ± 5	304 ± 5	315 ± 4
Na	ISO 16967	85 ± 1	202 ± 3	217 ± 2
P	ISO 16967	487 ± 7	831 ± 10	1133 ± 9
Si	ISO 16967	608 ± 25	2817 ± 35	7790 ± 114

[a] w.b.: wet basis.
[b] d.b.: dry basis.
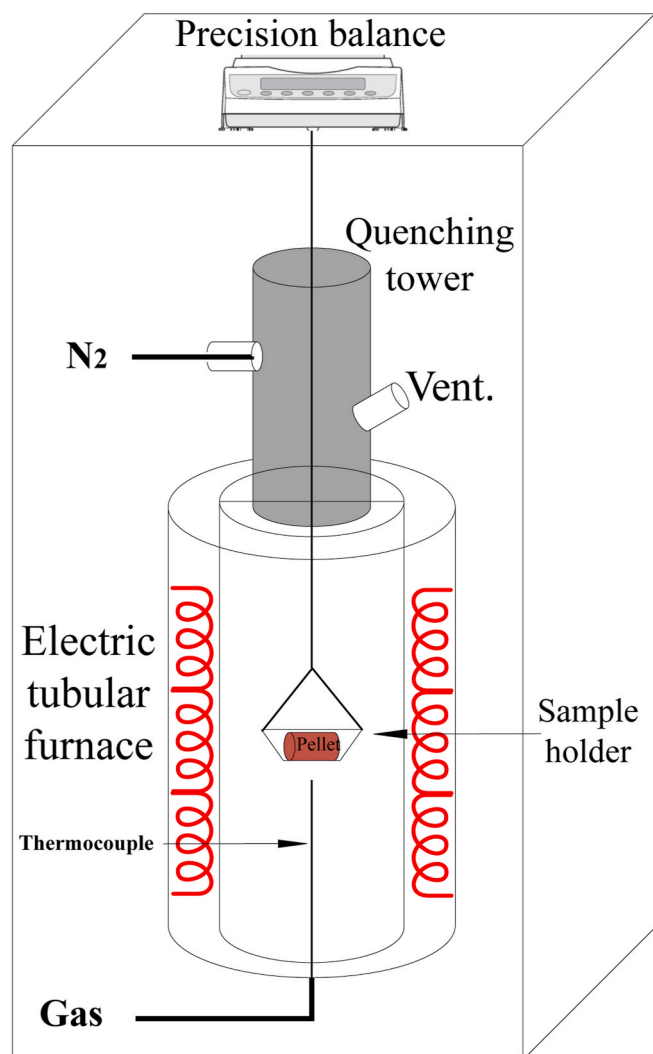
Fig. 1. Schematic sketch of the single pellet reactor (macro-TGA).

TGA) used for the fuel conversion experiments. This reactor is well-described in a previous study [30]. The fuel conversion experiments were carried out at different furnace temperatures (600, 800, 950 °C) with a predetermined atmosphere (65 vol% N_2, 20 vol% CO_2, 15 vol% H_2O). After the devolatilization stage; this gas atmosphere is intended to simulate a transition phase from devolatilization to the char gasification step.

The total flow rate of gases was 7 normal liters per minute. A single pellet (~ 700 mg) was manually lowered down into the heating zone typically in 2–3 s by using a sample holder made of platinum woven mesh (~ 32 mesh per centimeter, and a wire diameter of 0.076 mm). To investigate the ash transformations at different stages of thermal conversion, each sample was quenched in N_2 at three different conversion times: 1) BD: before devolatilization (i.e., at 80% of full devolatilization time) 2) AD: after devolatilization (i.e., at 10% of full char conversion

time), to observe the effect of the surrounding atmosphere and 3) AFC: after the full char conversion stage to observe the effect of prolonged char conversion time on the release of K and P. The method used for the calculation of the time for each stage was described in more detail elsewhere [31]. Twelve replicates (i.e., 12 individual single pellets experiments) were performed for each experimental condition. Table 2 shows the fuel conversion time needed to reach each stage. The char conversion at the furnace temperature of 600 °C was very slow under the specified gaseous environment; therefore, only the BD and AD samples were considered for characterization at this temperature.

Elemental analysis was performed on six collected char/ash residues. SEM-EDS and XRD analyses were performed on the remaining char/ash residues.

2.3. ICP and IC

Inductively coupled plasma-optical emission spectroscopy (ICP-OES; Spectro Arcos SOP) was applied based on ISO 16967 and ISO 16968 standards following microwave-assisted pressurized total acid digestion (Anton Paar, Multiwave PRO) to determine the major ash-forming elements in the fuels and the collected residues. Ion chromatography (IC; Shimadzu LC 20) was used to determine the chlorine content in the fuels, chars, and ash residues after bomb digestion according to ISO 16994 and in predominantly inorganic residues after aqueous leaching.

2.4. Elemental release quantification

The releases of K and P from the fuels were quantified by mass balance calculations based on the produced char and ash. This method is described in detail in previous studies [14,32]. For quantification of the release (R_i), the following equation was used:

$$R_i = 100 \times \left(1 - \frac{m_{residue}}{m_{fuel}\left(1 - C_{moisture}^{fuel}\right)} \times \frac{C_i^{residue}(d.b.)}{C_i^{fuel}(d.b.)} \right)$$

where $m_{residue}$ and m_{fuel} are the mass of the collected char/ash residue and the mass of the fuel fed to the Macro-TGA reactor, respectively. $C_{moisture}^{fuel}$, C_i^{fuel}, and $C_i^{residue}$ are the concentrations of moisture and element i in the fuel and the concentration of element i in the collected char/ash residue, respectively. The standard deviation of the release data was calculated from the standard deviations in the measurements of elemental compositions of the fuels.

2.5. SEM-EDS

A scanning electron microscope (SEM) (Jeol JSM-IT300), equipped with an Oxford energy dispersive X-ray spectroscopy (EDS) detector, was used to study morphology and elemental composition of the fuel and the collected char and ash residues. The powder prepared from the collected residues at different thermal conversion stages were placed on a carbon tape attached to aluminum sample holders. The backscattered electron detector was used to find the inorganic matter in the residues. For bulk elemental composition, an area analysis (350 × 475 μm) at two positions per sample was performed using the EDS-mapping technique. For the elemental compositions of melted structures and most recurrent individual particles, such as included minerals, at least ten spot analyses

Table 2

Fuel conversion time (in seconds) needed to reach each studied stage, i.e., before devolatilization (BD), after devolatilization (AD), and after full char conversion (AFC).

Sample	600 °C			800 °C			950 °C		
	BD	AD	AFC	BD	AD	AFC	BD	AD	AFC
Bark	64	258	n.a.	35	89	3295	16	38	888
Twigs	74	288	n.a.	37	120	8122	22	80	1020
Bark+Twigs	68	270	n.a.	35	105	6000	20	60	1310

n.a. = not analyzed.

were performed by EDS-point technique, and the average composition is reported.

2.6. P-XRD

In order to identify and quantify the crystalline phases and to estimate the amount of amorphous phases in the collected residues, powder X-ray diffraction (P-XRD) technique with a Si low-background sample holder was used. A Panalytical Empyrean instrument with copper tube was used for obtaining X-ray diffraction patterns. For the quantification of the crystalline phases, the Rietveld method was used with the aid of the HighScore Plus 4.8 software [33]. Databases used in this study are the PAN-ICSD database [34] and PDF-4+ 2019 databases [35]. The K-factor method was used to quantify the amorphous phases [36,37].

2.7. TECs

Thermochemical equilibrium calculations (TECs) were applied to find which phases may be stable under the experimental conditions and to interpret the experimental results in order to suggest ash transformation paths. In this study, TECs were performed by using the Equilib module of FactSage 7.2 [38] with FactPS (for gas and stoichiometric solid phases) and FToxid+FTsalt (oxide and salt solution phases) databases simultaneously. Table 3 shows the selected databases for TECs. The initial input was based on the analysis of the fuels listed in Table 1. Only elements with concentrations higher than 0.01 wt% in the fuel were taken into account in the TECs. In order to simulate the gaseous atmosphere, the partial pressures of CO_2, and H_2O, i.e., 0.2 and 0.15 atm, respectively, were fixed. The resulting partial pressure of O_2 was calculated based on the experimental temperature. Subsequently, a global equilibrium modeling approach was employed (using the elemental composition of the respective fuels as input, including both the organic and inorganic fractions) to predict the co-existing phases under the influence of the abovementioned gas atmosphere.

3. Results

3.1. Concentration of ash-forming elements in char and ash residues and release quantification of K and P

Fig. 2 shows the concentration of ash-forming elements in the studied forest residues at different fuel conversion stages and furnace temperatures. The concentrations of S and Cl were very low in the obtained char-ash residues, which indicates that the majority of S and Cl was released from the char-ash residue during fuel conversion. The produced char from bark, i.e., the residues obtained shortly before devolatilization (BD) and after devolatilization (AD), were dominated by Ca and K and, to a lesser extent, Mg, Si, and P. The produced char from twigs was dominated by Si, Ca, and K and, to a lesser extent, P and Mg. The char produced from twigs have much higher Si, K, and P, but lower Ca than that produced from bark. The concentrations of most of the ash-forming

elements in the char produced from bark+twigs were intermediate between those produced from bark and twigs separately. In general, increasing fuel conversion time and increasing temperatures caused an increased concentration of all main ash-forming elements (except Cl and S) in the produced char.

The effects of different temperatures and conversion times on the K and P release from the studied forest residues are shown in Fig. 3. Low release of K (<12%) and P (<16%) was observed for all fuels, and no significant differences could be seen between BD and AD except for twigs at 600 °C. In general, for bark and twigs, the main release of K and P occurred during the devolatilization stage. Increasing temperature from 600 °C to 950 °C did not significantly affect the release of K and P during devolatilization. For the bark and twigs mixture, the main fraction of the total K release occurred during char conversion. In comparison to the other fuels, the total P release from twigs+bark was only about half. Although the char conversion (gasification) time is extended beyond BD, the K and P release did not increase significantly, which is shown by comparing the results between BD, AD, and AFC samples (see Fig. 3). A decreased char yield at an extended char conversion time beyond BD (see Fig. 4), contributed to higher concentrations of K and P in the produced char.

3.2. Fuel characterization

Different inorganic matters distributed heterogeneously throughout the fuels are shown in SEM micrographs presented in Fig. 5. Based on EDS and XRD results, the Ca-rich pseudo-cubic particles observed in the SEM for all fuels were calcium oxalate monohydrate ($CaC_2O_4H_2O$). Calcium oxalates are the main Ca storage source in forest-based biomass and are more abundant in the bark than in the stem wood [15,39]. Si-rich areas could also be seen in SEM micrographs of twigs and bark+twigs, and those are most probably amorphous hydrated silica deposited as phytoliths in the fuel.

3.3. Char residues characterization

Similar to the fuels, different inorganic matters distributed heterogeneously throughout the chars were observed by SEM. These can be the same inorganic matters as found in the untreated fuels, or as decomposed compounds originating from those, or as precipitated salts. One representative micrograph of each fuel at different conditions are shown in Fig. 6 and Fig. 7. Distinct pseudo-cubic particles that are similar to those found in the fuels were found in all char residues. The amount and the size of these particles are larger in the char produced from bark. These particles, which mainly consist of calcium oxalates at BD, are completely decomposed to $CaCO_3$ at AD (see Tables 4 and 5). Shortly after devolatilization at higher temperatures (≥800 °C), a low fraction of $CaCO_3$ was decomposed to CaO. The SiO_2 found in the char of twigs and bark+twigs probably formed as a result of the dehydration of phytoliths during devolatilization. For all fuels, no crystalline compound containing K and P could be detected in the char. According to the SEM-EDS analysis, those elements were evenly distributed in the char. The SEM-EDS analysis also showed areas rich in Si and Ca in the char from twigs.

3.4. Ash characterization

Ashes produced from the fuels at different furnace temperatures seem to have partially melted, see Fig. 8. The melted structures found in the ashes produced at 800 °C and 950 °C from the bark were rich in Ca and K and, to less extent Mg. Based on XRD results presented in Table 6, a significant part of the ash samples contains crystalline phases dominated by Ca- and Ca/K carbonates and hydroxyapatite. In ash produced at 950 °C, CaO is also detected in the sample.

The molten structures found in the ashes produced at 800 °C and 950 °C from twigs were rich in Si, Ca, and K, and, to lesser extents, P and Mg. A major part of the ash samples (>75 wt%) is in the amorphous

Table 3
The selected databases for the TECs.

Database	Full name solution
FactPS	Pure stoichiometric gas and solid phases
FToxid	Slag A (liquid oxide melt): K_2O, SiO_2, CaO, MgO, P_2O_5, …
	MeO: Monoxide Rocksalt-str. Fe(2), Ca, Ba, Mg, Ni, Co, Mn(2); dilute Zn, Al, Cr, Fe(3), Mn(3);
	Bred: Bredigite $Ca_3(Ca,Mg)_4Mg(SiO_4)_4$ – a solid solution originating from $Ca_7Mg(SiO_4)_4$ by substitution of some Ca by Mg.
	Wollastonite, $CaSiO3$
	cPyr: Clinopyroxene (Ca,Sr,Mg,Fe,Ni,Zn,Mn,Na)[Mg,Ni,Zn,Mn,Fe, Fe^{3+}·Al]>Al,Fe^{3+},Si<SiO_6
FTSalt	LCSO: (K^+,Ca^{2+}//CO_3^{2-},SO_4^{2-} melt)
	SCSO: K,[Ca]//CO_3,SO_4(ss) solid solution
	CSOB: [Li],Na,K//SO_4,CO_3(ss) low lithium content solid solution.

Fig. 2. Concentration of ash-forming main elements in fuel, char obtained before devolatilization (BD) and after devolatilization (AD), and ash obtained after char conversion (AFC): (a) and (b) bark, (c) and (d) twigs, and (e) and (f) bark+twigs.

phase (see Table 6). The crystalline part in the ash sample produced at 800 °C was dominated by Ca carbonate, Ca silicate, and hydroxyapatite. At 950 °C, the crystalline part of the produced ash sample was dominated by Ca and Ca-Mg silicates, hydroxyapatite, and carbonated hydroxyapatite. Compared to twigs, the ash residues from bark+twigs were less sintered. The amount of amorphous phase in the produced ash residues from bark+twigs was around 60 wt%, which was higher than

for bark but lower than for twigs. In ash samples produced at a furnace temperature of 800 °C, K was not found in the crystalline part of the ash. In samples produced at 950 °C, K was found as K-Ca carbonates, most probably due to the solidification of a K-Ca rich carbonate melt, and in amorphous phases. Based on XRD results, the only P crystalline phase found is hydroxyapatite. At higher furnace temperature, the amount of hydroxyapatite decreases in the produced ash samples.
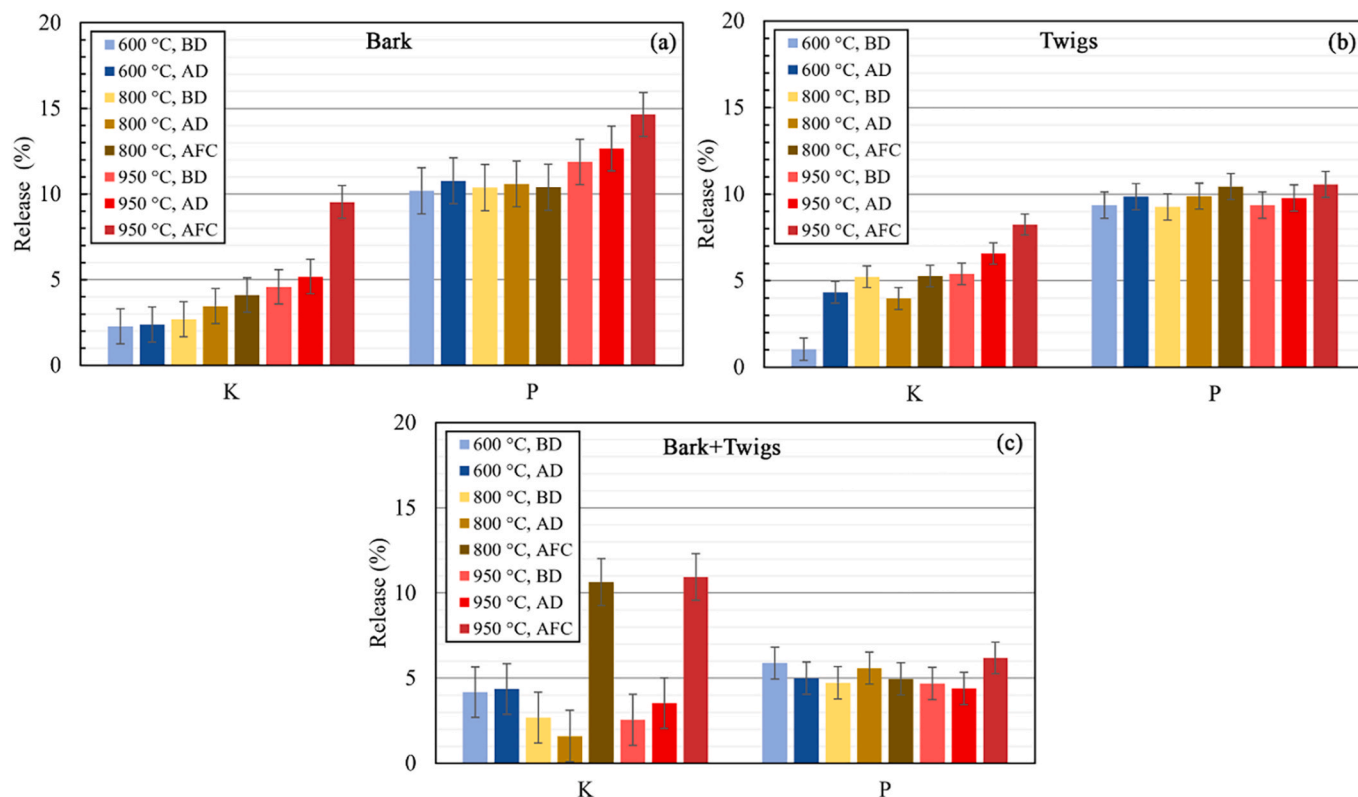
Fig. 3. Release of K and P after different fuel conversion stages (i.e., before devolatilization (BD), after devolatilization (AD), and after char conversion (AFC)) at different furnace temperatures (a) bark, (b) twigs, and (c) bark+twigs.
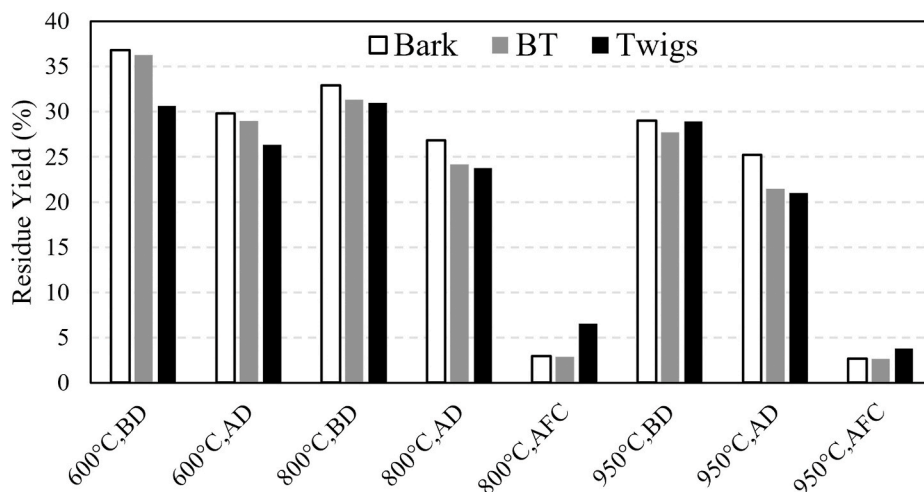
Fig. 4. Resulting yields (wt.% d.b.) of produced char/ash from bark, twigs, and bark+twigs (BT) after each fuel conversion stages, i.e., before devolatilization (BD), after devolatilization (AD), and after char conversion (AFC).

3.5. TECs

The distribution of predicted condensed phases calculated by TECs in the temperature range 600–1000 °C is shown in Fig. 9. For bark at low temperature, the predicted condensed phases are dominated by Ca- and Ca-K carbonates. At temperatures above 800 °C, a carbonate melt rich in Ca and K is predicted to form. By increasing the temperature from 800 °C to 950 °C, a fraction of the carbonate melt decomposes to CaO. Hydroxyapatite is the only stable compound containing P within the studied temperature range.

For twigs at low temperatures, $K_2Si_2O_5$ and $K_2Si_4O_9$ are the main

compounds containing K. At higher temperatures (above 750 °C) a silicate melt rich in K is formed. Similar to the bark, P is predicted to form hydroxyapatite for the twigs sample.

The predicted condensed phases for bark+twigs are different than for both bark and twigs. At low temperatures, K_2CO_3 and $K_2Si_2O_5$ are the main K containing compounds. A silicate melt rich in K is predicted to form in a narrow temperature range (780–810 °C). At a temperature above 880 °C, K is found both in carbonate and a silicate-phosphate melt rich in K and Ca. Below 900 °C, hydroxyapatite is the only P containing compound while above 900 °C, P is found in a silicate-phosphate melt rich in K and Ca.
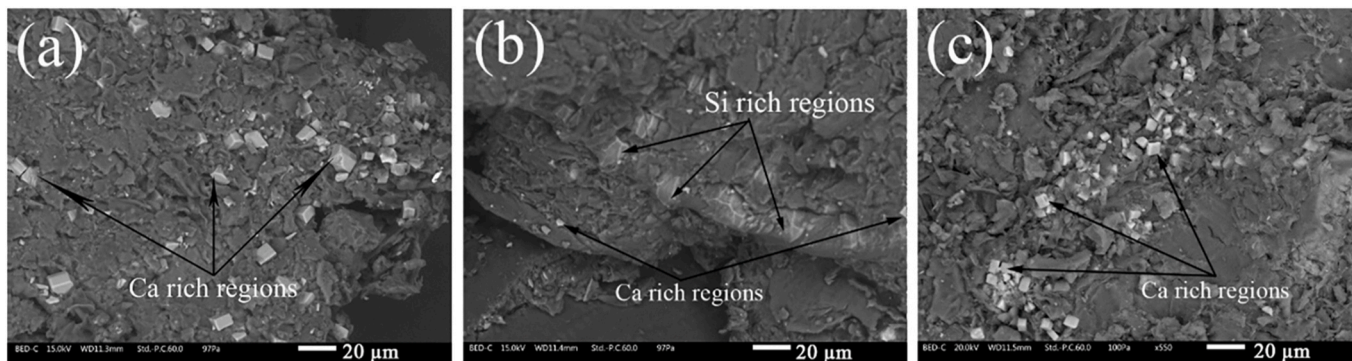
Fig. 5. Backscattered SEM micrographs of untreated fuels; (a) bark, (b) twigs, and (c) bark+twigs.
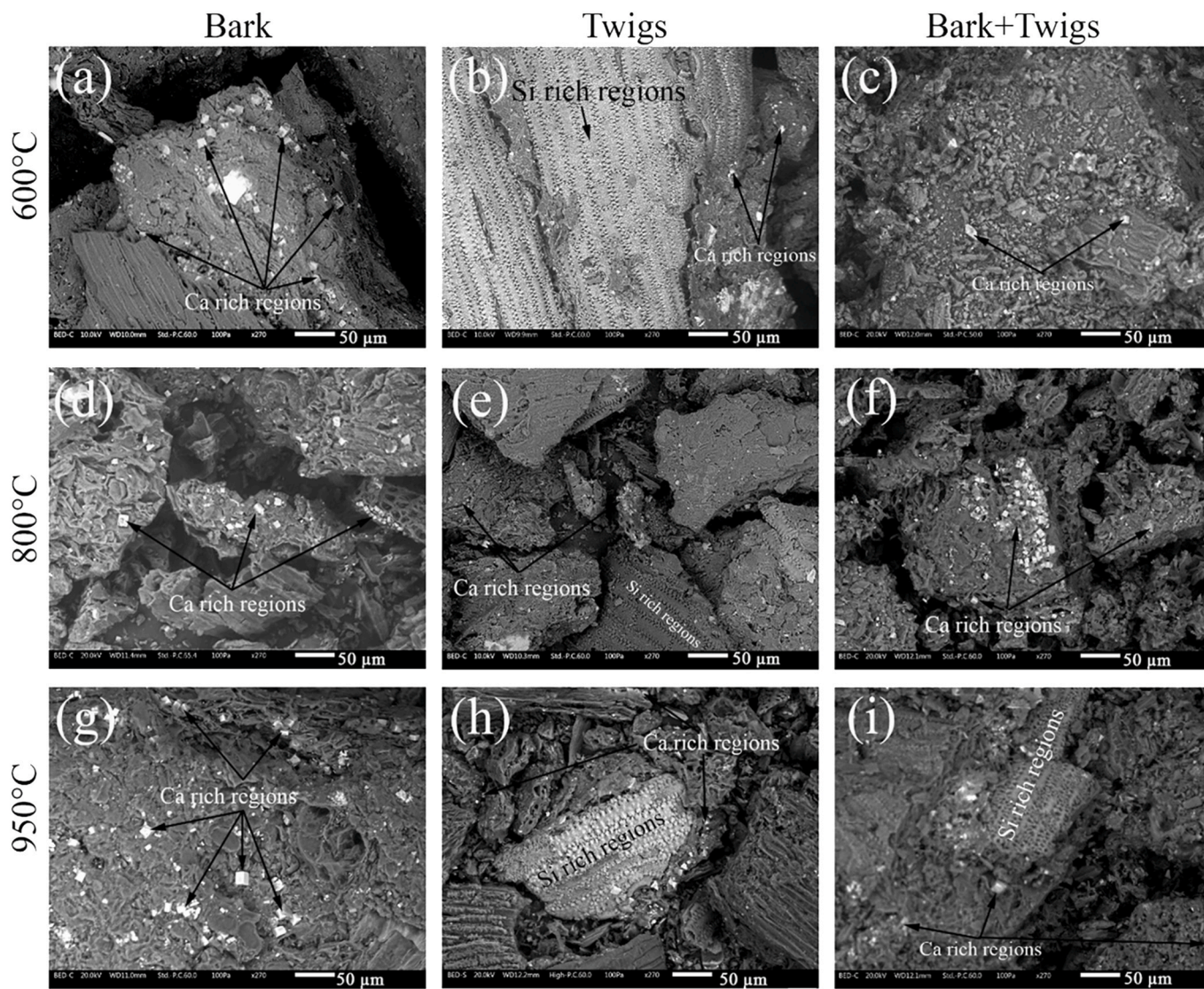
Fig. 6. Backscattered SEM micrographs of char residues from BD (i.e., before devolatilization) at different furnace temperatures; (a,d,g) bark, (b,e,h) twigs, and (c,f, i) bark+twigs.
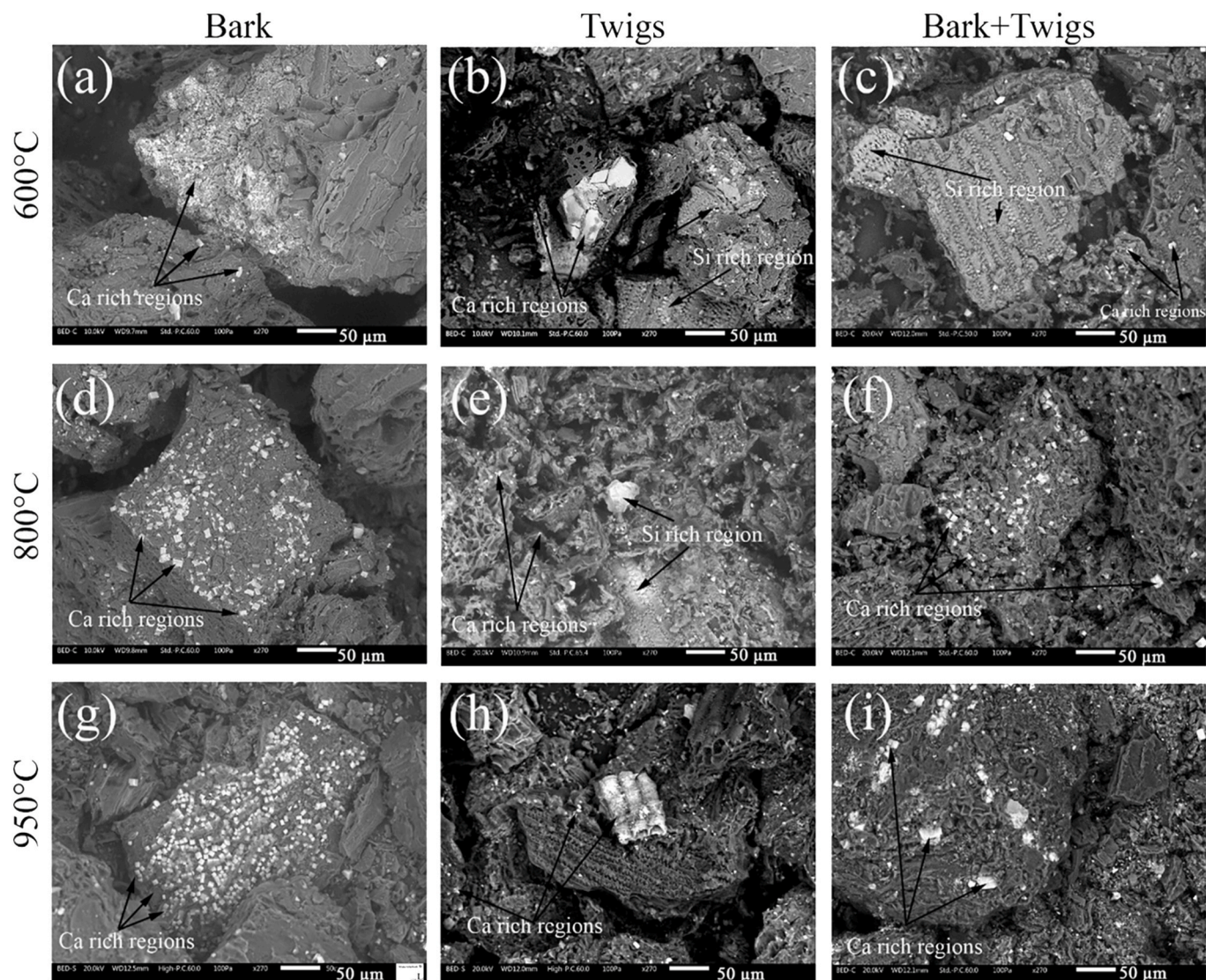
Fig. 7. Backscattered SEM micrographs of char residues from AD (i.e., after devolatilization) at different furnace temperatures (a,d,g) bark, (b,e,h) twigs, and (c,f, i) bark+twigs.

Table 4
Crystalline phases and amorphous phase (in wt.%) identified by XRD in samples produced from bark, twigs, and bark+twigs (BT) at different furnace temperatures before devolatilization (BD).

Phase	600 °C			800 °C			950 °C		
Chemical formula (mineral)	Bark	BT	Twigs	Bark	BT	Twigs	Bark	BT	Twigs
$CaC_2O_4.H_2O$ (Whewellite)	17	14	9	9	15	9	11	6	7
$CaCO_3$ (Calcite)	4	1	6	13	3	7	17	11	11
SiO_2		1	2		1	3		2	3
Amorphous[a]	79	84	73	78	81	81	72	81	75

[a] Amorphous organic and inorganic phases, a significant share of the amorphous phase is derived from the char.

4. Discussion

4.1. Ash transformation with a focus on K and P

4.1.1. Bark (Ca-K-rich fuel with a minor amount of P)

Only a small fraction of the K (<6%) and P (<14%) was released during the devolatilization stage, probably due to the low availability of organically-associated K and P in bark (K and P is mostly present in a water-soluble form such as K_2HPO_4/KH_2PO_4, KCl, and K_2SO_4) [16,40]. Due to the formation of stable condensed compounds, the release of K and P is low during char gasification. Therefore, the main fraction of K and P in the bark is found in the residual ash. In agreement with TECs and previous studies [21,24,31,41], results showed that during char gasification, K and P species mainly react with Ca species (organically bound Ca-compounds and $CaCO_3$ originated from Ca−oxalate) to form stable K-Ca carbonates and hydroxyapatite, respectively. As previously shown [41], the formation of K-Ca carbonate melt during char conversion may cause an even lower K release since a fraction of K was captured or surrounded by the melt. Therefore, the observed very low release of K during char gasification at 800 °C could also be related to

Table 5
Crystalline phases and amorphous phase (in wt.%) identified by XRD in samples produced from bark, twigs, and bark+twigs (BT) at different furnace temperatures shortly after devolatilization (AD).

Phase	600 °C			800 °C			950 °C		
Chemical formula (mineral)	Bark	BT	Twigs	Bark	BT	Twigs	Bark	BT	Twigs
$CaCO_3$ (Calcite)	27	20	19	29	22	23	14	16	17
$MgCO_3$ (Magnesite)									1
CaO (Lime)							5	5	4
$CaOH$ (Portlandite)							6		
SiO_2		3	4		2	4		3	3
Amorphous[a]	73	77	76	71	76	73	75	76	75

[a] Amorphous organic and inorganic phases, a significant share of the amorphous phase is derived from the char.
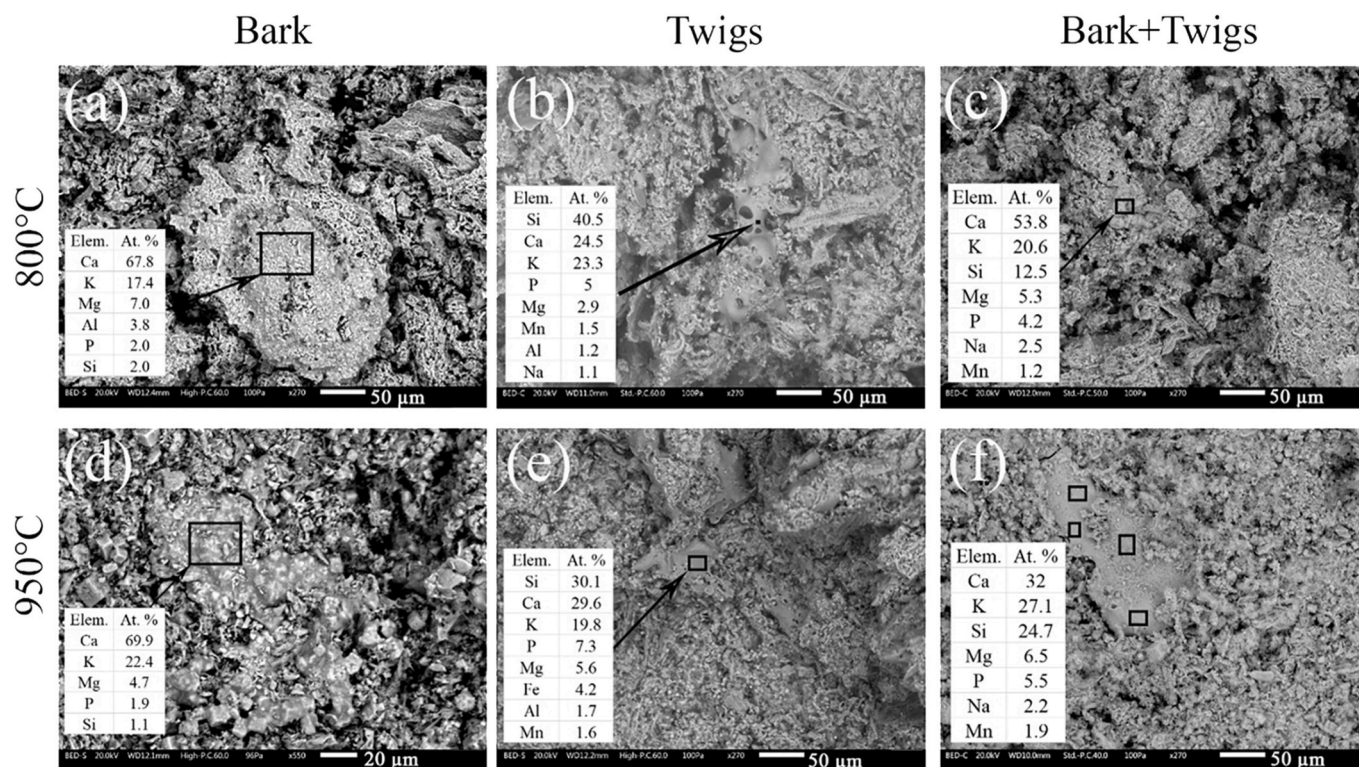
Fig. 8. Backscattered SEM micrographs of ash produced from bark (a, d), twigs (b, e), and bark+twigs (c, f) at different furnace temperatures, and average elemental composition of molten structured areas as determined by EDS-area analysis.

Table 6
Crystalline phases and amorphous phase (in wt.%) identified by XRD in the ash samples produced from bark, twigs, and bark+twigs (BT) at different furnace temperatures.

Phase	800 °C			950 °C		
Chemical Formula (Mineral)	Bark	BT	Twigs	Bark	BT	Twigs
$CaCO_3$ (Calcite)	27		9	30	10	
$(Ca_{0.845}Mg_{0.155})(CO_3)$	3	9				
$K_2Ca(CO_3)_2$ (Fairchildite)				13	7	
$K_2Ca_2(CO_3)_3$	13					
CaO (Lime)				9	6	1
$CaOH$ (Portlandite)				5	9	
$CaSiO_3$ (Wollastonite)						8
Ca_2SiO_4		14	8			
$Ca_2Mg(Si_2O_7)$						3
$Ca_5(SiO_4)_2(CO_3)$		7				
$Ca_5(PO_4)_3OH$ (Apatite)	10	10	4	8	7	7
$Ca_{10}(PO_4)_{5.65}(CO_3)_{0.64}(OH)_{3.452}$						2
Amorphous	47	60	76	35	61	79

K-Ca carbonate melt formation (see Fig. 8a and d). At 800 °C, K was found in a crystalline phase of $K_2Ca_2(CO_3)_3$ in the ash. At higher furnace temperature, i.e., 950 °C, a low fraction of K was released, and CaO formed due to the dissociation of the Ca-K-rich carbonate melt and Ca-carbonate originating from the Ca oxalates. During solidification, K was found in $K_2Ca(CO_3)_2$ that likely forms from the melt.

4.1.2. Twigs (Si-Ca-K-rich fuel with relatively high amount of P)

Like the bark, a small fraction of the K ($<7\%$) and P ($<11\%$) in twigs was released during the devolatilization stage, probably due to the low availability of organically-associated K and P. Also, for this fuel, the K and P release were low during char gasification, and the main fractions of these elements were found in the residual ash. In comparison with bark, residual ash from twigs contained a higher amount of amorphous phases, probably due to the higher Si content in the twigs, which cause to form amorphous K rich silicates during char conversion. Results showed that during char gasification, K species mainly react with Si species (amorphous silica) and Ca species (organically bound Ca-compounds and $CaCO_3$ originated from Ca−oxalate) to form K-Ca rich silicates. Similar to the bark, during char gasification, results showed that P species mainly react with Ca species to form hydroxyapatite, in
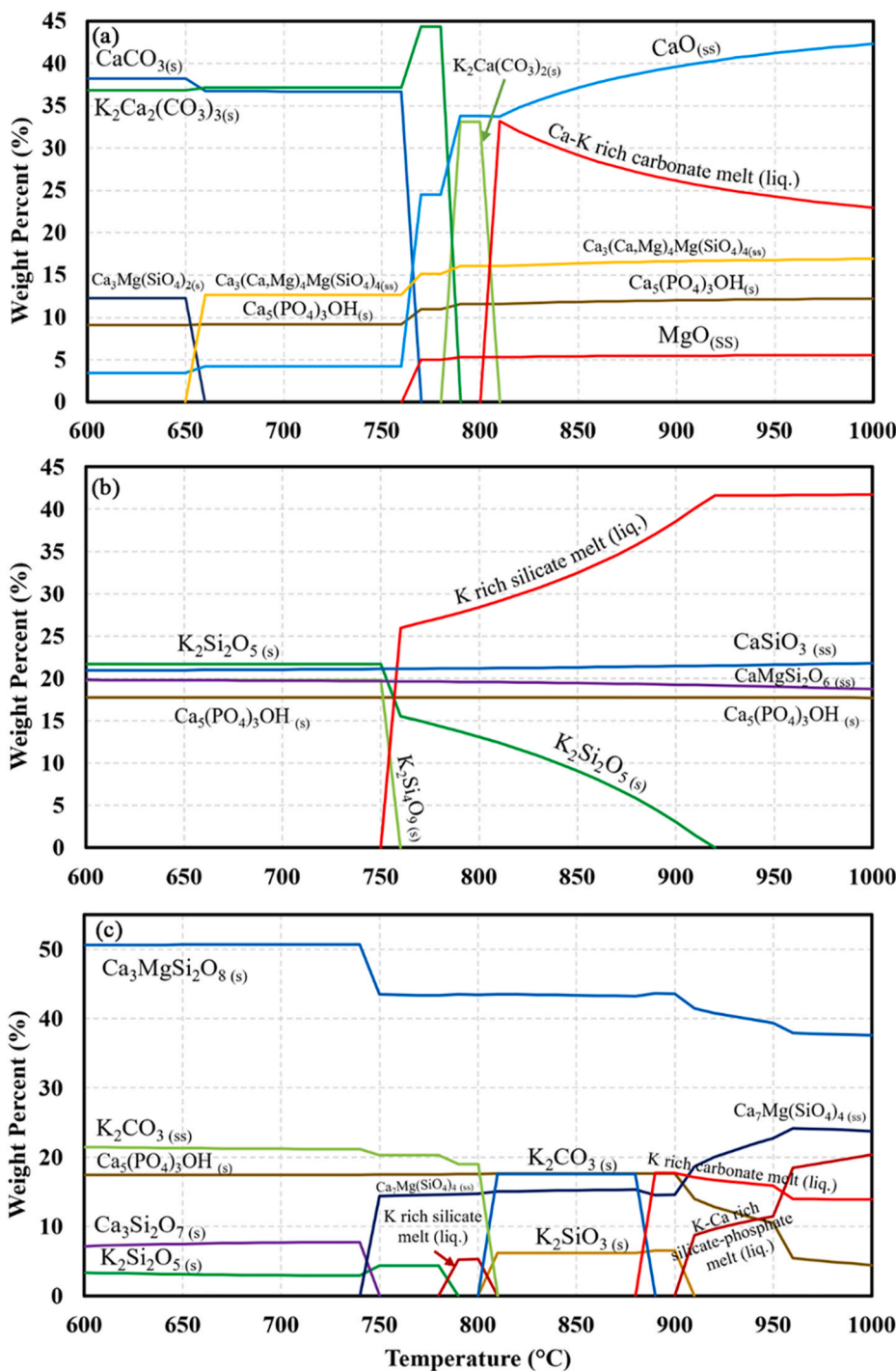
Fig. 9. Distribution of predicted condensed phases calculated by TECs; (a) bark, (b) twigs, and (c) bark+twigs.

agreement with TECs.

4.1.3. Bark and twigs mixture (Ca-K-Si rich fuel with a moderate amount of P)

In opposite to twigs and bark individually, the majority of K release occurred during char conversion. One possibility to the higher release of K during the char conversion, could be that initially formed K-rich silicates react with the additional Ca species added via the bark fuel to form Ca-K rich silicates. As suggested by the results of this study and other studies [42–45], the interaction of alkaline earth metals with K-silicates enhances the release of K to the gas phase to some extent. By mixing twigs and bark, the total P release was approximately half of the total P

release from twigs and bark individually. Similar to the bark and twigs, during char gasification, results showed that P species mainly react with Ca species to form hydroxyapatite, in agreement with TECs. The observed lower release of P during the char conversion of the bark and twig mixture might be related to the increase of the probability and possibility of interaction between P found mainly in the twigs with the extra Ca added via the bark fuel.

4.2. Practical implications

The produced char from the studied forest residues had considerably higher concentrations of K and P compared to typical metallurgical coke,
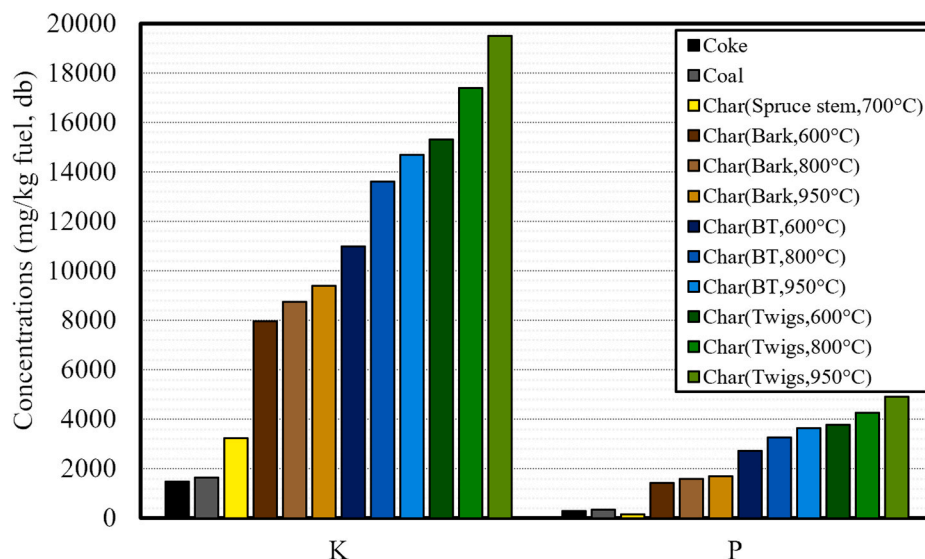
Fig. 10. Concentration of K and P in the different char samples produced/taken directly after devolatilization (AD), in char produced from stem wood (data extracted from Phounglamcheik et al. [40]) and in typical coal and coke used as fuel and reducing agents in blast furnaces (data extracted from Suopajärvi et al. [1]).

pulverized coal, and also char produced from stem wood (see Fig. 10). The release of these elements was low even at the highest studied temperature and not significantly affected by an extension of the char conversion time. The observed low release for K and P was due to the formation of stable condensed compounds within the whole studied temperature range (600–950 °C).

The results from this study show that a release of approx. 80% for K and P is needed to produce chars from non-stem wood-based forest residues that are comparable to typical coal and coke used today in the metallurgical industry. This is probably very hard to reach in pyrolysis and gasification processes at temperatures below 1000 °C. Even though the results in this study are based on single-pellet studies in lab-scale environment, even lower levels of K and P release are expected in industrial-scale plants. The released fraction of K and P from one char particle can react with the ash constitutes and/or char matrix formed in other char particles, thereby being retained in the produced char through secondary reactions [17]. A selection or pre-treatment of the biomass-based raw materials used to produce char for metallurgical applications may, therefore, be needed to avoid the increase of K and P input to the metallurgical processes. Since the majority of K and P (~75%) in forest residues are leachable by water [16,46], a leaching step using water or another solvents [47] could be a potential pre-treatment process before pyrolysis [46]. Also the novel technique of combining NIR and X-ray to differentiate between exogenous and naturally embedded ash-forming elements may be of use to define the possibilities to reduce harmful elements by different pre-treatments [48].

5. Conclusions

Ash transformation and release of K and P during the single-pellet conversion of different types of forest residues (i.e., bark, twigs, and bark+twigs) were investigated at different furnace temperatures (i.e., 600, 800, and 950 °C) and within and after different fuel conversion stages, i.e., shortly before and after full devolatilization and char gasification.

- A low amount of P and K (less than 16%) were released from all fuels at all studied temperatures. The main release of P for all fuels occurred during the devolatilization stage. The main release of K also occurred during the devolatilization stage for all fuels, except for the

mixture of twigs and bark, where the main release occurred during the char conversion stage.
- The concentrations of K and P in the produced char were more than four times higher than that in typical coke and pulverized coal that are usually used in metallurgical processes. Increasing conversion (processing) time, i.e., increased the mass losses of char, caused an increase of K and P concentrations in the char.
- The char residues from all fuels obtained shortly after devolatilization were dominated by Ca carbonates. K and P were evenly distributed within the char residues, and no crystalline compounds containing K and P were found.
- K in ash residues of bark was found in $K_2Ca_2(CO_3)_3$, and $K_2Ca(CO_3)_2$. K in ash residues from twigs and bark+twigs was mainly found in the amorphous part of ash, most likely in the form of K-Ca rich silicates. Hydroxyapatite was found as the main P crystalline compound in all ash residues at all furnace temperatures.
- Estimations show that a release of more than 80% is needed for typical bark and forest residues assortments to reach concentrations of K and P that are typical of blast furnace coals and cokes. The results from this study show that K and P mostly form stable condensed phases when using forest residues at temperatures below 950 °C. Therefore, the use of forest residues in slow pyrolysis processes and low-temperature gasification processes will probably not enable the release required to reach K and P concentrations that are comparable to the coal and fossil coke used today in steel and iron production.

References

[1] H. Suopajärvi, K. Umeki, E. Mousa, A. Hedayati, H. Romar, A. Kemppainen, C. Wang, A. Phounglamcheik, S. Tuomikoski, N. Norberg, A. Andefors, M. Öhman, U. Lassi, T. Fabritius, Use of biomass in integrated steelmaking – status quo, future needs and comparison to other low-CO2 steel production technologies, Appl. Energy 213 (2018) 384–407.

[2] A. Babich, D. Senk, J. Solar, I. de Marco, Efficiency of biomass use for blast furnace injection, ISIJ Int. 59 (12) (2019) 2212–2219.

[3] J. van Dam, The Charcoal Transition: Greening the Charcoal Value Chain to Mitigate Climate Change and Improve Local Livelihoods, Food and Agriculture Organization of the United Nations, Rome, Italy, 2017.

[4] I. Agirre, T. Griessacher, G. Rösler, J. Antrekowitsch, Production of charcoal as an alternative reducing agent from agricultural residues using a semi-continuous semi-pilot scale pyrolysis screw reactor, Fuel Process. Technol. 106 (2013) 114–121.

[5] M.U. Babler, A. Phounglamcheik, M. Amovic, R. Ljunggren, K. Engvall, Modeling and pilot plant runs of slow biomass pyrolysis in a rotary kiln, Appl. Energy 207 (2017) 123–133.

[6] M. Dastidar, B. Sarkar, M. Mitra, Effect of alkali on different iron making processes, MOJ Mining Met 1 (3) (2018) 89–98.

[7] L. Bai, J. Zhang, H. Guo, X.-S. Zhang, X.-D. Zhang, Circulation and enrichment of alkali metal in blast furnace, J. Iron Steel Res. Int. 9 (2008).

[8] I. Iwasaki, E. Fregeau-Wu, T. Fujita, Removal of phosphorus from steelmaking slags: a literature survey, Miner. Process. Extr. Metall. Rev. 12 (1) (1993) 19–36.

[9] S. Basu, S. Seetharaman, A.K. Lahiri, Thermodynamics of phosphorus and sulphur removal during basic oxygen steelmaking, Steel Res. Int. 81 (11) (2010) 932–939.

[10] H. Suopajärvi, E. Pongrácz, T. Fabritius, The potential of using biomass-based reducing agents in the blast furnace: a review of thermochemical conversion technologies and assessments related to sustainability, Renew. Sustain. Energy Rev. 25 (2013) 511–528.

[11] J. Lampreia, M.S.M. de Araújo, C.P. de Campos, M.A.V. Freitas, L.P. Rosa, R. Solari, C. Gesteira, R. Ribas, N.F. Silva, Analyses and perspectives for Brazilian low carbon technological development in the energy sector, Renew. Sustain. Energy Rev. 15 (7) (2011) 3432–3444.

[12] K.L. Kenney, W.A. Smith, G.L. Gresham, T.L. Westover, Understanding biomass feedstock variability, Biofuels 4 (1) (2013) 111–127.

[13] K.C. Badgujar, B.M. Bhanage, in: T. Bhaskar, A. Pandey, S.V. Mohan, D.-J. Lee, S. K. Khanal (Eds.), Chapter 1 - Dedicated and Waste Feedstocks for Biorefinery: an Approach to Develop a Sustainable Society, Waste Biorefinery, Elsevier, 2018, pp. 3–38.

[14] S.C. van Lith, V. Alonso-Ramírez, P.A. Jensen, F.J. Frandsen, P. Glarborg, Release to the gas phase of inorganic elements during wood combustion. Part 1: development and evaluation of quantification methods, Energy Fuels 20 (3) (2006) 964–978.

[15] J. Werkelin, Ash-forming Elements and Their Chemical Forms in Woody Biomass Fuels, 2008.

[16] J. Werkelin, B.-J. Skrifvars, M. Zevenhoven, B. Holmbom, M. Hupa, Chemical forms of ash-forming elements in woody biomass fuels, Fuel 89 (2) (2010) 481–493.

[17] S.C. van Lith, P.A. Jensen, F.J. Frandsen, P. Glarborg, Release to the gas phase of inorganic elements during wood combustion. Part 2: influence of fuel composition, Energy Fuels 22 (3) (2008) 1598–1609.

[18] K. Davidsson, B. Stojkova, J. Pettersson, Alkali emission from birchwood particles during rapid pyrolysis, Energy Fuels 16 (5) (2002) 1033–1039.

[19] K. Davidsson, J. Korsgren, J. Pettersson, U. Jäglid, The effects of fuel washing techniques on alkali release from biomass, Fuel 81 (2) (2002) 137–142.

[20] L. Wang, A. Moilanen, J. Lehtinen, J. Konttinen, B.G. Matas, Release of potassium during devolatilization of spruce bark, Energy Procedia 105 (2017) 1295–1301.

[21] D. Boström, N. Skoglund, A. Grimm, C. Boman, M. Ohman, M. Broström, R. Backman, Ash transformation chemistry during combustion of biomass, Energy Fuels 26 (1) (2012) 85–93.

[22] M. Díaz-Ramírez, C. Boman, F. Sebastián, J. Royo, S. Xiong, D. Boström, Ash characterization and transformation behavior of the fixed-bed combustion of novel crops: poplar, brassica, and cassava fuels, Energy Fuels 26 (6) (2012) 3218–3229.

[23] J. Fagerström, E. Steinvall, D. Boström, C. Boman, Alkali transformation during single pellet combustion of soft wood and wheat straw, Fuel Process. Technol. 143 (2016) 204–212.

[24] A. Strandberg, M. Carlborg, C. Boman, M. Broström, Ash transformation during single-pellet combustion of a silicon-poor woody biomass, Energy Fuels 33 (8) (2019) 7770–7777.

[25] A. Strandberg, N. Skoglund, M. Thyrel, T.A. Lestander, M. Broström, R. Backman, Time-resolved study of silicate slag formation during combustion of wheat straw pellets, Energy Fuels 33 (3) (2019) 2308–2318.

[26] H. Wu, M. Castro, P.A. Jensen, F.J. Frandsen, P. Glarborg, K. Dam-Johansen, M. Røkke, K. Lundtorp, Release and transformation of inorganic elements in combustion of a high-phosphorus fuel, Energy Fuels 25 (7) (2011) 2874–2886.

[27] P.A. Tchoffor, F. Moradian, A. Pettersson, K.O. Davidsson, H. Thunman, Influence of Fuel Ash Characteristics on the Release of Potassium, Chlorine, and Sulfur from Biomass Fuels under Steam-Fluidized Bed Gasification Conditions, Energy Fuels, 2016.

[28] H.-b. Zhao, Q. Song, X.-y. Wu, Q. Yao, Transformation of alkali and alkaline earth metallic species during pyrolysis and CO2 gasification of rice straw char, J. Fuel Chem. Technol. 46 (1) (2018) 27–33.

[29] T. Yang, K. Jia, X. Kai, Y. Sun, Y. Li, R. Li, A study on the migration behavior of K, Na, and Cl during biomass gasification, BioResources 11 (3) (2016) 7133–7144.

[30] A. Phounglamcheik, T. Wretborn, K. Umeki, Increasing efficiency of charcoal production with bio-oil recycling, Energy Fuels 32 (9) (2018) 9650–9658.

[31] A. Hedayati, H. Sefidari, C. Boman, N. Skoglund, N. Kienzl, M. Öhman, Ash transformation during single-pellet gasification of agricultural biomass with focus on potassium and phosphorus, Fuel Process. Technol. 217 (2021), 106805.

[32] S.C. van Lith, in: P.A. Jensen, F. Frandsen, P. Glarborg (Eds.), Release of Inorganic Elements during Wood-Firing on a Grate, 2006.

[33] M.S.T. Degen, E. Bron, U. König, G. Nénert, The HighScore suite, Powder Diffr. 29 (December 2014) S13–S18.

[34] The Inorganic Crystal Structure Database (ICSD), FIZ Karlsruhe 2015-1, Karlsruhe, Germany.

[35] PDF-4+, Database, International Centre for Diffraction Data, Newtown Square, PA, USA, 2020.

[36] B.H. O'Connor, M. Raven, Application of the Rietveld refinement procedure in assaying powdered mixtures, J. Powder Diffraction 3 (1) (1988) 2–6.

[37] A. Adibhatla, S. Speakman, T. Degen, Rietveld Amorphous Quantification without Pain: the K-Factor Approach, 2014.

[38] C.W. Bale, E. Bélisle, P. Chartrand, S.A. Decterov, G. Eriksson, A.E. Gheribi, K. Hack, I.H. Jung, Y.B. Kang, J. Melançon, A.D. Pelton, S. Petersen, C. Robelin, J. Sangster, P. Spencer, M.A. Van Ende, FactSage thermochemical software and databases, Calphad 54 (2016) (2010–2016) 35–53.

[39] F. Rees, F. Watteau, S. Mathieu, M.-P. Turpault, Y. Le Brech, R. Qiu, J.L. Morel, Metal immobilization on wood-derived biochars: distribution and reactivity of carbonate phases, J. Environ. Qual. 46 (4) (2017) 845–854.

[40] M. Zevenhoven, P. Yrjas, B.-J. Skrifvars, M. Hupa, Characterization of ash-forming matter in various solid fuels by selective leaching and its implications for fluidized-bed combustion, Energy Fuels 26 (10) (2012) 6366–6386.

[41] A. Hedayati, R. Lindgren, N. Skoglund, C. Boman, N. Kienzl, M. Öhman, Ash transformation during single-pellet combustion of agricultural biomass with a focus on potassium and phosphorus, Energy Fuels 35 (2) (2021) 1449–1464.

[42] P. Thy, C. Lesher, B.M. Jenkins, Experimental determination of high-temperature elemental losses from biomass slag, Fuel 79 (6) (2000) 693–700.

[43] I.-L. Näzelius, J. Fagerström, C. Boman, D. Boström, M. Öhman, Slagging in fixed-bed combustion of phosphorus-poor biomass: critical ash-forming processes and compositions, Energy Fuels 29 (2) (2015) 894–908.

[44] C. Gilbe, M. Ohman, E. Lindström, D. Boström, R. Backman, R. Samuelsson, J. Burvall, Slagging characteristics during residential combustion of biomass pellets, Energy Fuels 22 (5) (2008) 3536–3543.

[45] A. Novaković, S.C. van Lith, F.J. Frandsen, P.A. Jensen, L.B. Holgersen, Release of potassium from the systems K−Ca−Si and K−Ca−P, Energy Fuels 23 (7) (2009) 3423–3428.

[46] Q. He, J. Yu, X. Song, L. Ding, J. Wei, G. Yu, Utilization of biomass ash for upgrading petroleum coke gasification: effect of soluble and insoluble components, Energy 192 (2020), 116642.

[47] M.T. Reza, R. Emerson, M.H. Uddin, G. Gresham, C.J. Coronella, Ash reduction of corn stover by mild hydrothermal preprocessing, Biomass Conver. Biorefinery 5 (1) (2015) 21–31.

[48] M. Thyrel, R. Aulin, T.A. Lestander, A method for differentiating between exogenous and naturally embedded ash in bio-based feedstock by combining ED-XRF and NIR spectroscopy, Biomass Bioenergy 122 (2019) 84–89.